molecular pharmaceutics

Article

pubs.acs.org/molecularpharmaceutics

Metabolic Profile, Enzyme Kinetics, and Reaction Phenotyping of β-Lapachone Metabolism in Human Liver and Intestine in Vitro

Xuefang Cheng, Fang Liu, Tingting Yan, Xueyan Zhou, Liang Wu, Ke Liao, Guangji Wang,* and Haiping Hao*

State Key Laboratory of Natural Medicines, Key Lab of Drug Metabolism and Pharmacokinetics, China Pharmaceutical University, Nanjing, China

ABSTRACT: β-Lapachone (β-Lap) is an NAD(P)H:quinone oxidoreductase 1 (NQO1) target antitumor drug candidate in phase II clinical trials. The present study aimed to uncover the metabolic profile, enzyme kinetics, and enzyme isoforms for the metabolism of β-Lap in human liver and intestine in vitro. NQO1-mediated quinone reduction and subsequent glucuronidation is the predominant metabolic pathway for β-Lap in humans; a pair of regioisomers (M1 and M2) of reduced β-Lap glucuronides were the major metabolites found from human S9 incubations. The overall glucuronidation clearance of β-Lap in human liver S9 was 4754.90 μL/min/mg of protein and was 8.1-fold of that in human intestinal S9. Recombinant UDP-glucuronosyltransferase (UGT) screening, correlation analysis, enzyme kinetics, and chemical inhibition study were performed to determine the UGT isoforms involved in β-Lap metabolism. UGT1A7, UGT1A8, and UGT1A9 are the predominant isoforms responsible for the formation of M2 while UGT2B7 is the main isoform for M1, suggesting a regioselective glucuronidation of reduced quinone by UGTs. It was of interest to find that β-Lap underwent nonenzymatic two-electron reduction, providing a novel explanation for the toxicities of β-Lap to NQO1-negative cells at high concentration and with long-time incubation. In conclusion, this study contributes to a better understanding of not only β-Lap metabolism but its antitumor property as well.

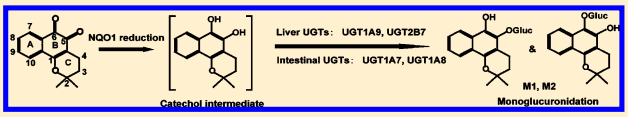

KEYWORDS: *glucuronidation, UGT, enzyme kinetics, reaction phenotyping, β-lapachone*

INTRODUCTION

β-Lapachone (3,4-dihydro-2,2-dimethyl-2*H*-naphthol[1,2-*b*]-pyran-5,6-dione, β-Lap), an *o*-naphthoquinone derivative originally obtained from the bark of the lapacho tree (Tabebuia avellanedae) in South America,[1] has aroused huge attention for its widely pharmacological activities including antibacterial,[2] antifungal,[3] trypanocidal,[4,5] and especially the powerful anticancer potentials.[6] β-Lap as a novel anticancer agent exhibits selective antitumor activity against various human cancers.[7−10] It is currently in multiple phase II clinical trials as monotherapy and in combination with other cytotoxic drugs, such as gemcitabine in pancreatic adenocarcinoma treatment.[11,12] Accumulating evidence strongly suggests that the anticancer effect of β-Lap originates from the metabolic bioactivation by NQO1.[13] NQO1-mediated futile cycling between the oxidized and reduced forms of β-Lap results in dramatic reactive oxygen species (ROS) formation, extensive DNA damage, poly(ADP-ribose) polymerase-1 (PARP-1) hyperactivation, and ATP and NAD+ loss, leading to cell death.[10,14] NQO1 is thus believed to be the primary intracellular target of β-Lap, and accumulating evidence indicates that the pharmacological efficacy of β-Lap is largely dependent on its metabolic process. Therefore, it is definitely important to understand the metabolic characteristics and mechanisms of β-Lap in humans, which provide a translational link from its metabolism to the pharmacological efficacies.

Identification of metabolites of β-Lap had been previously performed both in vivo and in vitro and in animal species and human beings. Except for the specific oxidation metabolism in red blood cells, β-Lap was found predominantly metabolized via ortho-quinone two electron reduction and sequentially various types of phase II conjugations.[12,15,16] However, largely unknown are the enzyme kinetics and enzyme isoforms involved in the metabolism of β-Lap, both of which are indispensable parts of drug metabolism research. In addition, given that the pharmacological efficacies of β-Lap are closely related to its metabolic process, enzyme kinetics and enzyme reaction phenotyping study are important for a better understanding and prediction of potential individual variability of its pharmacological efficacies. In a more recent study, we have developed a universally applicable method for the reaction phenotyping assay of sequential quinone reduction and glucuronidation of ortho-quinone compounds using tanshinone IIA as a model compound.[17] Because β-Lap is structurally similar to tanshinone IIA, we hypothesized herein that β-Lap may also be metabolized predominantly via an NQO1 and UGT catalyzed sequential metabolism.

The present study was thus designed to clarify the metabolic profiles of β-Lap in human liver and intestinal S9 fractions, to identify the UGT isoform(s) responsible for the metabolism of β-Lap in humans, and to determine the glucuronidation enzyme kinetics of β-Lap in pooled human liver, intestinal S9 and recombinant human UGTs. Because NQO1 is mainly distributed

Received: May 29, 2012
Revised: October 8, 2012
Accepted: November 7, 2012
Published: November 7, 2012

in cytosol while UGTs are mainly located in microsomes, the S9 fractions that contain both cytosol and microsomes were applied in the present study for characterizing β-Lap enzyme kinetics.[17] Furthermore, recombinant human NQO1 was used in combination with human UGT supersomes to determine the sequential quinone reduction and subsequent conjugation metabolism.

MATERIALS AND METHODS

Materials. β-Lapachone was purchased from Southeast Pharmaceuticals, Inc. (Jiangsu, China). Glucose 6-phosphate, glucose 6-phosphate dehydrogenase (PDH), β-nicotinamide adenine dinucleotide phosphate (NADP), uridine 5′-diphosphate-glucuronic acid (UDPGA), D-saccharic acid 1,4-lactone, β-glucuronidase (*Escherichia coli*), recombinant human NQO1, alamethicin, dicoumarol, propofol, naloxone, naloxone-3-glucuronide, and serotonin were all purchased from Sigma Chemical (St. Louis, MO, USA). Diazepam was purchased from the National Institute for the Control of Pharmaceutical and Biological Products (Beijing, China). Pooled human liver S9 (HLS9), human intestinal S9 (HIS9), and human liver cytosol were obtained from Research Institute for Liver Diseases Co LTD (Shanghai, China). A panel of recombinant human UGT Supersomes expressed in baculovirus infected insect cells (UGT1A1, 1A3, 1A4, 1A6, 1A7, 1A8, 1A9, 1A10, 2B4, 2B7, 2B15, and 2B17) and 7 individual human liver microsomes (HH61, HH629, HH854, HH855, HH645, HH746, and HH524) with the data on UGT activities toward β-estradiol, trifluoperazine, and propofol were obtained from BD Biosciences (Bedford, MA, USA). Oasia HLB solid phase cartridges were obtained from Waters Corporation (Milford, MA, USA). All other chemicals were of HPLC grade or the best grade that was commercially available.

Metabolic Profiling. The typical reaction mixtures (200 μL) contained 100 mM potassium phosphate buffer (pH 7.4), 5 mM $MgCl_2$, 200 μg of S9 protein, a NADPH regenerating system (0.2 mM NADP, 1.9 mM glucose-6-phosphate, 1.2 U/mL glucose-6-phosphate dehydrogenase), 2 mM UDPGA, 1 mM saccharic acid 1,4-lactone, and 40 μM β-Lap. Control assay was conducted without β-Lap. The pooled subcellular fraction S9 was pretreated with alamethicin at 25 μg/mg of protein on ice for 20 min to diminish the latency of UGT activity. After preincubation for 5 min at 37 °C, the reaction was initiated by the addition of 2 mM UDPGA. All reactions were incubated at 37 °C for 2 h and terminated by cooling in ice bath followed by solid-phase extraction (SPE) and then analyzed by liquid chromatography/hybrid ion trap/time-of-flight mass spectrometry (LC-IT-TOF/MS).

Metabolite identification of β-Lap was performed by LC-IT-TOF/MS in both the positive and negative ionization modes with full-scan detection. LC experiments were conducted using a Shimadzu (Kyoto, Japan) HPLC system consisting of an LC-20AD binary pump, an SIL-20AC autosampler, a CTO-20AC column oven, and an SPD-M20A PDA. Chromatographic separation of analytes was achieved using a Zorbax Eclipse XDB-C18 column (150 mm × 2.1 mm i.d., 3.5 μm) with a guard column. The column and autosampler tray temperatures were set at 35 and 4 °C, respectively. The mobile phase consisted of water (A, 0.1% (v/v) formic acid) and acetonitrile (B) and was delivered at a flow rate of 0.2 mL/min. The mass detection was carried out using a Shimadzu ion trap/time-of-flight hybrid mass spectrometry (IT-TOF/MS) (Shimadzu, Kyoto, Japan), equipped with an electrospray ionization source. The optimized operating conditions were as follows: positive/negative mode; electrospray voltage, 4.5 kV (positive) and −3.5 kV (negative); CDL temperature, 200 °C; block heater temperature, 200 °C; nebulizing gas (N_2), 1.5 L/min; drying gas (N_2) pressure, 0.1 MPa; trap cooling gas (Ar) flow, 95 mL/min; pressure of ion trap, 1.7×10^{-2} Pa; pressure of TOF region, 1.5×10^{-4} Pa; ion accumulated time, 50 ms; detector voltage, 1.70 kV; collision energy at 30% for MS^2 and 50% for MS^3; scan range of m/z 100−800 for MS^1, 100−750 for MS^2, and 50−750 for MS^3. Data acquisition and analysis were performed with LC Solution 3.0 software (Shimadzu, Kyoto, Japan).

To identify the glucuronidation metabolites, the glucuronide hydrolysis assay was performed using β-glucuronidase. The incubation samples (200 μL) prepared as described above were immediately centrifuged (9000*g* for 10 min), and an aliquot (100 μL) of sample was incubated in the absence (control) and presence of 4000 units of β-D-glucuronidase in acetic acid/sodium acetate buffer (pH 4.5) for 6 h at 37 °C.

Dicoumarol, a specific inhibitor of NQO1,[18] was used to determine the potential role of NQO1 on β-Lap metabolism. To determine its inhibitory effect on the formation of M1 and M2, β-Lap (5 μM) was incubated with pooled human liver S9 (0.025 mg/mL) in the absence or presence of 20 μM dicoumarol for 10 min. For M3, M4, and M5, β-Lap (100 μM) was incubated with pooled human liver S9 (1 mg/mL) in the absence or presence of 100 μM dicoumarol for 2 h.

Reaction Phenotyping. Based on our previously developed method, pooled human liver cytosol (0.2 mg of protein/mL) as an NQO1 donor in combination with recombinant UGTs was applied for the reaction phenotyping screen. A panel of commercially available UGT isoforms including UGT 1A1, 1A3, 1A4, 1A6, 1A7, 1A8, 1A9, 1A10, 2B4, 2B7, 2B15, and 2B17 (protein concentrations were all at 0.05 mg/mL) was screened for β-Lap glucuronidation at two different concentrations (0.5 μM and 5 μM). The incubation conditions were the same as those described above for S9 incubations. The reaction was terminated with cold acetonitrile, and the supernatants were analyzed by LC−MS.

Correlation Analysis. The correlation analysis between the glucuronidation activity toward β-Lap and the typical UGT substrates in seven individual human liver microsomes was performed. Glucuronidation activities of estradiol 3β-glucuronidation (UGT1A1), trifluoperazine glucuronidation (UGT1A4), and propofol glucuronidation (UGT1A9) were obtained from the manufacturer. Naloxone glucuronidation (UGT2B7) was measured based on a previously reported method.[19] The incubation conditions were the same as described above for the glucuronidation assay of β-Lap. A linear regression analysis was conducted, and a p value less than 0.05 was considered statistically significant.

Chemical Inhibition Studies. To further verify the phenotyping results, chemical inhibition studies were performed using three typical UGT probe substrates, serotonin (UGT1A6), propofol (UGT1A9), and naloxone (UGT2B7). β-Lap (0.5 μM) was incubated with pooled HLS9 (0.025 mg/mL) in the absence or presence of each typical substrate (0−500 μM), and the IC50 value of each typical probe substrate was determined. The same incubation procedure as described above was followed.

Enzyme Kinetics Analysis. The enzyme kinetics assay for β-Lap (0.1−50 μM) glucuronidation was conducted in pooled human liver (0.025 mg/mL) and intestinal (0.1 mg/mL) S9 fractions, and the recombinant human UGT1A7 (0.008 mg/mL), UGT1A8 (0.025 mg/mL), UGT1A9 (0.005 mg/mL), and UGT2B7 (0.0125 mg/mL) in combination with a pooled human liver cytosol. The incubation time was all set at 10 min.

Table 1. Summary of Molecular Ions, Formula, Retention Time, and Fragment Ions for Metabolite Identification of β-Lap in Human Liver S9 Incubation System

metabolites	obsd m/z (ppm[a])	formula (M)	retention time (min)	molecular ions	fragment ions
M1, M2	419.1335 (−3.10)	$C_{21}H_{24}O_9$	37.16, 37.81	$[M - H]^-$	243.0997, 225.0895, 187.0389, 175.0252, 159.0455
M3	435.1289 (−1.84)	$C_{21}H_{24}O_{10}$	16.07	$[M - H]^-$	259.0936, 201.0537, 193.0337, 173.0624
M4	435.1279 (−4.41)	$C_{21}H_{24}O_{10}$	23.51	$[M - H]^-$	259.0934, 187.0386, 159.0418
M5	595.1615 (−8.91)	$C_{27}H_{32}O_{15}$	22.79	$[M - H]^-$	419.1312, 243.1053, 187.0342
M6	275.0910 (2.91)	$C_{15}H_{16}O_5$	24.75	$[M - H]^-$	231.1014, 187.1132, 129.0946
β-Lap	243.1013 (−1.23)	$C_{15}H_{14}O_3$	41.02	$[M + H]^+$	225.0900, 201.0563, 187.0397, 159.0440, 133.0296

[a]Difference between the observed and theoretical values.

The protein concentration and incubation time were preferentially optimized to ensure linear formation of metabolites. Other incubation conditions were the same as those described previously.

Enzymatic and Nonenzymatic Reduction of β-Lap. To determine the role of NQO1 on the metabolism of β-Lap, we used recombinant human NQO1 (50 μg/mL) in combination with recombinant UGT1A9 (0.05 mg/mL) or UGT2B7 (0.2 mg/mL) to determine the enzymatic and nonenzymatic reduction of β-Lap (20 μM). The following experimental groups were designed to compare their respective metabolic velocities: group 1 (with NQO1 and NADP); group 2 (with NQO1 and without NADP); group 3 (with NADP and without NQO1); group 4 (without NQO1 and NADP). The incubation time was 10 min for UGT1A9 and 15 min for UGT2B7. Other incubation conditions were the same as those described previously.

Quantification of β-Lap and β-Lap Glucuronides. The LC−MS analysis was performed using a Shimazu LC-10AD HPLC system, a SIL-HTC autosampler, and a CTO-10Avp column oven, which is coupled with a LC−MS 2010A quadrupole mass spectrometer equipped with an ESI interface (SHIMAZU, Japan).

The chromatographic separation was performed on a Zobax Eclipse XDB-C18 column (150 mm × 2.1 mm i.d., 3.5 μm) with a guard column. Samples were ionized using the following source conditions: gas flow, 1.5 L/min; curve dissolution line (CDL) voltage fixed as in tuning; CDL temperature, 250 °C; block temperature, 200 °C. The mobile phase consisted of water (A, 0.1% (v/v) formic acid) and acetonitrile (B). For the quantification of β-Lap, ESI positive ionization mass spectrometry operated in the selected ion monitoring (SIM) mode was applied using m/z 242.95. Diazepam (10 ng/mL) was used as an internal standard and monitored at m/z 284.95. The separation was achieved using the following elution gradient: linear gradient from 40% B to 90% B (0−1 min), and 90% B for another 3 min (1−4 min), then back to 40% B (4−5 min), and with the final stop at 9 min. For the determination of β-Lap glucuronides M1 and M2, ESI negative ionization mass spectrometry in SIM mode was applied with m/z 418.95 and the internal standard (chlorzoxazone, 20 ng/mL) at m/z 167.90. The separation was achieved using the following elution gradient: 30% B (0−2.5 min), linear gradient from 30% B to 38% B (2.5−14 min), 38% B to 90% B (14−15 min), 90% B for another 1.5 min (15−16.5 min), then back to 30% B (16.5−17 min), and finally with the stop at 21 min.

Because the authentic standards of β-Lap glucuronides were commercially unavailable, a β-D-glucuronidase hydrolysis method of "related quantitative coefficient" was developed for quantifying β-Lap glucuronides based on our previous method.[17] Using β-D-glucuronidase enzyme to hydrolyze the samples, β-Lap glucuronides were hydrolyzed to β-Lap because the catechol intermediate is highly unstable and immediately auto-oxidizes to β-Lap. The increased peak area of β-Lap of the hydrolyzed samples relative to the control samples (without the addition of β-D-glucuronidase enzyme) can be attributed to the

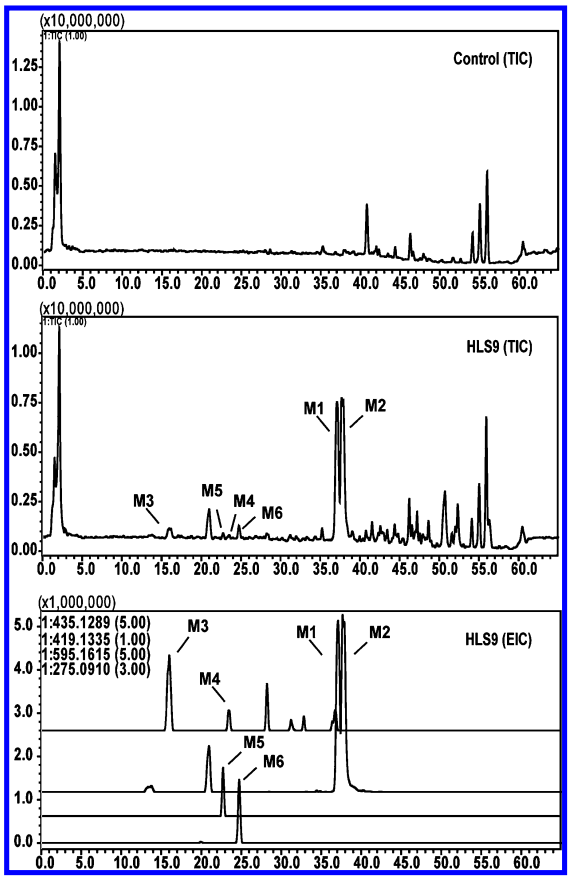

Figure 1. Total ion chromatograms (TIC) and extracted ion chromatograms (EIC) of β-Lap metabolites obtained from the negative ion scan mode. β-Lap was incubated with human liver S9 in the presence of NADPH-generating system and UDPGA at 37 °C for 2 h.

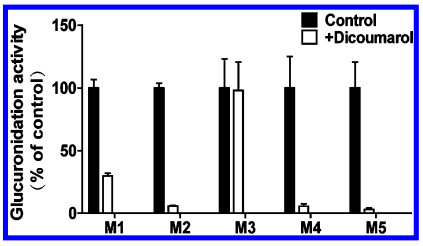

Figure 2. Inhibitory effect of dicoumarol on the formation of β-Lap glucuronides (M1, M2, M3, M4, and M5) in human liver S9 incubation system.

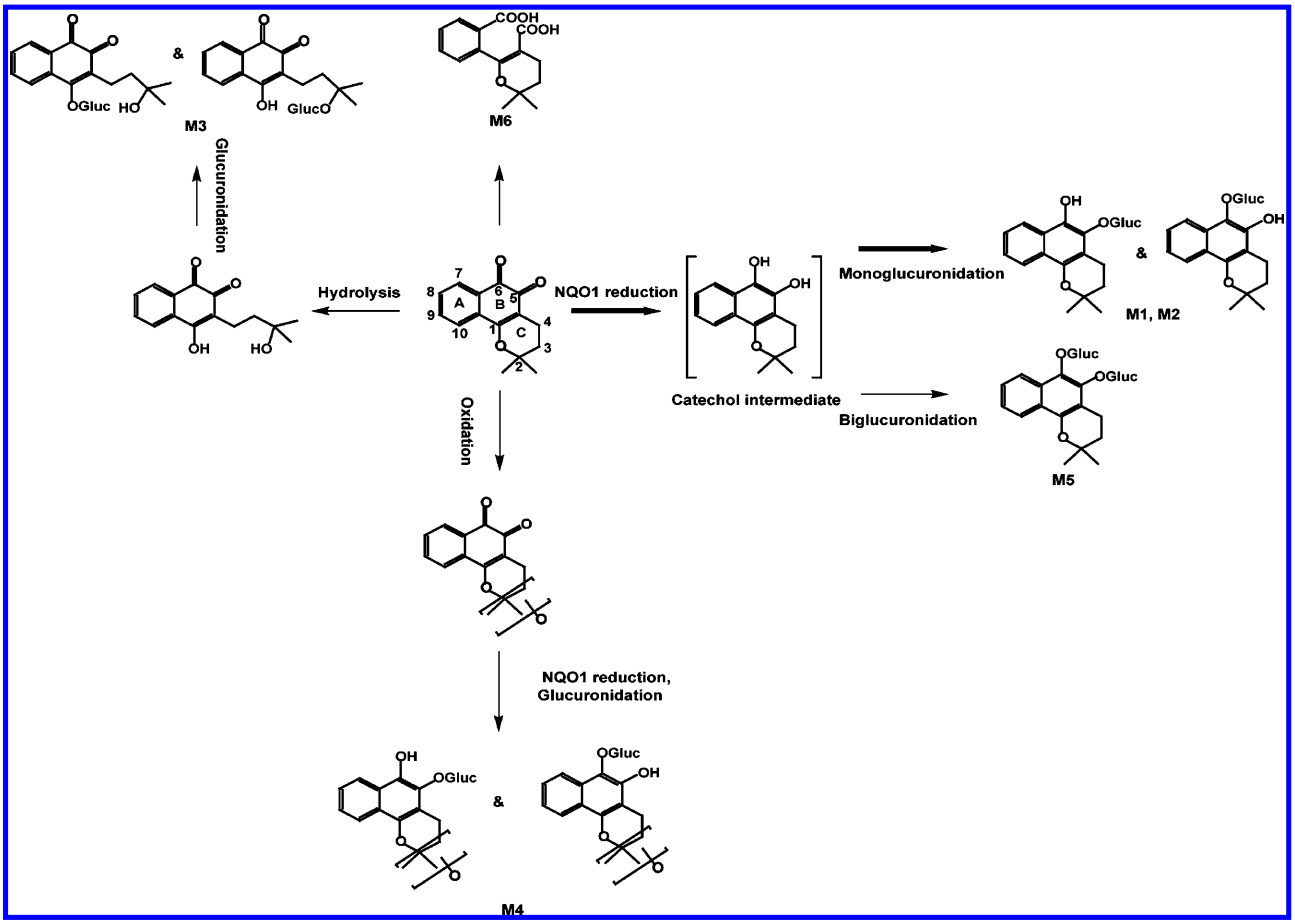

Figure 3. Proposed metabolic profile of β-Lap in human liver S9 fraction. Bold arrow "→" indicates the predominant metabolic pathway. The catechol intermediate produced from NQO1 mediated two-electron reduction was highly unstable and could not be detected.

release of β-Lap from both glucuronides (M1 and M2). The "related quantitative coefficient" was then determined by comparing the peak area of β-Lap released from the hydrolysis with that of β-Lap glucuronides, assuming M1 and M2 share the same mass response. The retention time of M1, M2, chlorzoxazone, β-Lap, and diazepam was 11.78, 12.43, 5.31, 5.33, and 5.38 min, respectively. The method for the quantification of β-Lap exhibited good linear response in a concentration range from 0.01 to 5 μM with a correlation coefficient over 0.994. The lower limit of quantification was 0.01 μM. The extraction recovery of β-Lap was determined to be over 85% at all tested concentrations and samples. The intrabatch accuracy ranged from 91.6 to 110.1% at the tested concentrations with the precision (RSD) within 5.0% for control samples, and 89.4–106.7% with the precision (RSD) within 6.3% for hydrolysis samples. The interbath accuracy ranged from 91.6% to 112.6% at the tested concentrations with the precision (RSD) within 5.4% for control samples, and from 88.8 to 109.1% with the precision (RSD) within 6.5% for hydrolysis samples.

Data Analysis. Metabolic rate was expressed as pmol/min/mg of protein. The formation of β-Lap glucuronides M1 and M2 in the pooled human liver or intestinal S9 fractions and in the human recombinant UGT1A7, UGT1A8, UGT1A9, and UGT2B7 expressed in baculovirus-infected cells was fitted to the substrate inhibition kinetics. The substrate inhibition Michaelis–Menten equation, $V = V_{max}[S]/(K_m + [S] + [S]^2/K_{si})$, where K_m is the Michaelis–Menten constant, V_{max} is the maximum velocity, [S] is the substrate concentration, and K_{si} is the inhibition constant for the second substrate molecule, was applied to estimate the apparent kinetic parameters using a nonlinear least-squares method. The correlation study was conducted by the Spearman correlation analysis, and the correlation was considered significant at the 0.05 level. Kinetic parameters, IC50, and K_{si} values are reported as means ± standard deviation.

RESULTS

Metabolic Profile of β-Lap in Human Liver and Intestinal S9 Fractions. A total of six metabolites including five glucuronidation products and a phase I oxidation metabolite were identified from human liver S9 fractions using LC-IT-TOF/MS analysis (Table 1, Figure 1). M1 and M2 ($[M - H]^-$, m/z 419.1335) were identified from both human liver and intestinal S9 fractions as a pair of regioisomers of the monoglucuronide of reduced β-Lap. As seen from Figure 1, M1 and M2 show the highest mass signal intensity among all the metabolites detected, indicating M1 and M2 are the major metabolites of β-Lap. M5 (m/z 595.1615) was identified as a diglucuronide product of the reduced β-Lap. M6 (m/z 275.0910), detected from both human liver and intestinal S9 fractions, was identified as a dicarboxylic acid metabolite, which was evidenced from the diagnostic fragment ions at m/z 231 and 187 generated from the precursor ion m/z 275 via sequential losses of CO_2.[12,15] M3 and M4 were identified as two novel metabolites from a sequential hydroxylation and glucuronidation of

β-Lap. The presence of the deprotonated ion at m/z 435 and the major fragment at m/z 259 implies that the glucuronidation may occur on either the catechol form of the oxidized β-Lap (NQO1 dependent) or the hydroxyl group after pyran ring hydrolysis (NQO1 independent). For M3, the fragment ion at m/z 201 was produced through a neutral loss of isopropanol (58 Da) from m/z 259; a further neutral loss of CO (28 Da) from m/z 201 produced an ion at m/z 173; this fragmental pattern indicates the hydroxylation may occur at the C2 position. In addition, dicoumarol showed negligible inhibitory effect on M3 formation (Figure 2), which indicates the glucuronidation must occur on the hydroxyl group after pyran ring hydrolysis. The formation of M4 was inhibited by dicoumarol to a great extent (Figure 2), indicating an NQO1 dependent manner; the production of a fragment at m/z 187 indicates the hydroxyl group from oxidation was lost together with the isobutene moiety (72 Da). Thus we proposed that M4 was produced from a hydroxylation metabolism at either position 3 or the dimethyl group and the subsequent glucuronidation at the catechol form of the reduced β-Lap. Dicoumarol inhibition experiments (Figure 2) in combination with β-glucuronidase enzyme hydrolysis (data not shown) demonstrate that NQO1-mediated quinone reduction and the subsequent glucuronidation is the predominant metabolic pathway for β-Lap, and a pair of regioisomers (M1 and M2) of reduced β-Lap glucuronides were the major metabolites in humans (Figure 3).

Reaction Phenotyping of β-Lap Glucuronidation. Incubation of β-Lap (0.5 and 5 μM) with 12 human UGT supersomes in combination with human liver cytosol as an NQO1 donor revealed that UGT1A7, UGT1A8, and UGT1A9 were the major isoforms involved in the formation of M2; the metabolic velocity at the β-Lap concentration of 5 μM was 11706.60, 4449.89, and 11702.20 pmol/min/mg, respectively. UGT2B7 was found to be the predominant isoform responsible for M1 production with a metabolic velocity at 4461.10 pmol/min/mg. All other UGT isoforms showed little activity (Figure 4).

Correlation Analysis with UGT Probe Substrates in Individual Human Liver Microsomes (HLMs). The velocities of producing M1 and M2 in 7 individual HLMs in combination with pooled human liver cytosol as an NQO1 donor ranged from 245.80 to 466.10 and 732.14 to 1754.98 pmol/min/mg of protein, respectively. The formation of M1 and M2 was correlated with the glucuronidation of estradiol at the 3-OH position (UGT1A1), trifluoperazine (UGT1A4), propofol (UGT1A9), and naloxone (UGT2B7) (Figure 5). M2 formation was found correlated well (r = 0.9421, p = 0.0015) with the glucuronidation of propofol, a typical UGT1A9 substrate. In contrast, no significant correlation was found with estradiol 3β-glucuronidation (UGT1A1) and naloxone glucuronidation (UGT2B7). Good correlation was observed between M2 formation and trifluoperazine glucuronidation (UGT1A4) that also has a good correlation with propofol glucuronidation (data from BD Biosciences). M1 formation only correlated well (r = 0.6633, p = 0.1043) with naloxone glucuronidation (UGT2B7). The results of correlation analysis further support the aforementioned reaction phenotyping results.

Inhibition of β-Lap Glucuronidation by UGT Probe Substrates. The inhibitory effects of three commonly used UGT probe substrates, serotonin (UGT1A6), propofol (UGT1A9), and naloxone (UGT2B7), on β-Lap glucuronidation activities in the pooled human liver S9 are shown in Figure 6. These substrates exhibited different inhibitory influences on the formation of β-Lap glucuronides in vitro. Propofol showed

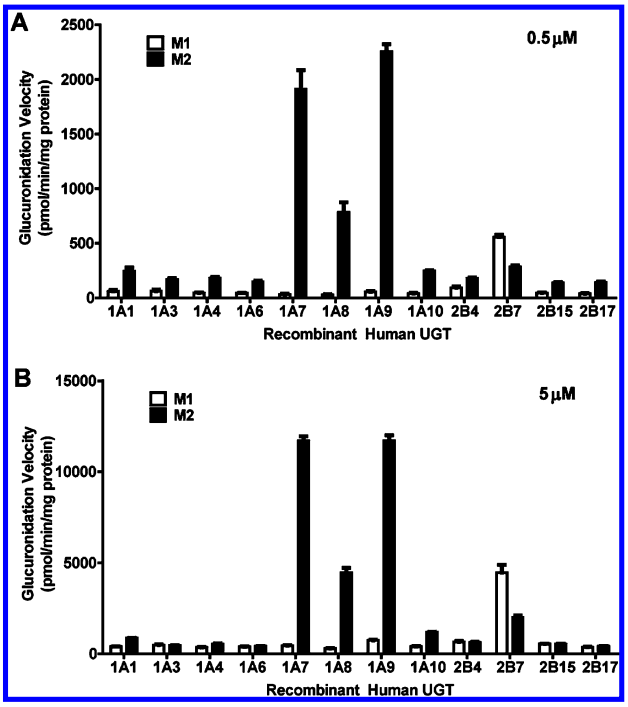

Figure 4. Formation of β-Lap glucuronides M1 and M2 by recombinant human UGT isoforms. 0.5 μM β-Lap (A) and 5 μM β-Lap (B) were incubated with recombinant human UGT isoforms (UGT 1A1, 1A3, 1A4, 1A6, 1A7, 1A8, 1A9, 1A10, 2B4, 2B7, 2B15, and 2B17) at 0.05 mg/mL protein for 10 min, using pooled human liver cytosol as an NQO1 donor as described in Materials and Methods. Open and closed columns represent β-Lap glucuronides M1 and M2, respectively. Each bar represents the mean ± SD of triplicate determinations.

potent inhibitory effect on both M1 and M2 formation, characterized with an IC50 value of 60.53 ± 1.04 μM and 91.75 ± 1.02 μM, respectively. Naloxone was shown to be a potent inhibitor of M1 formation, with an IC50 value of 104.20 ± 1.17 μM. Serotonin showed negligible inhibitory effect on both M1 and M2 formation with an IC50 > 500 μM.

Enzyme Kinetics Parameters. We performed the enzyme kinetics analysis of β-Lap glucuronidation in human liver and intestinal S9 fractions, and recombinant UGT1A7, UGT1A8, UGT1A9, and UGT2B7 in combination with a human liver cytosol incubation system. As shown in Figure 7 and Figure 8, kinetic data for HIS9, HLS9, UGT1A7, UGT1A8, UGT1A9, and UGT2B7 were best fitted to the substrate inhibition equation. Kinetic parameters including the apparent K_m, K_{si}, V_{max}, and CL_{int} (V_{max}/K_m) for M1 and M2 are summarized in Table 2. Substrate inhibition was strong in the formation of M1 catalyzed by UGT1A9 and UGT2B7 ($K_{si} \ll K_m$), but weak in others ($K_{si} \gg K_m$). For HLS9, the apparent kinetic parameter K_m, V_{max}, K_{si}, and CL_{int} for M1 was 2.37 ± 0.67 μM, 299.40 ± 46.53 pmol/min/mg, 17.07 ± 5.37 μM, and 126.33 μL/min/mg; and 0.28 ± 0.02 μM, 1296.00 ± 23.50 pmol/min/mg, 68.43 ± 6.31 μM, and 4628.57 μL/min/mg for M2, respectively. HIS9 could catalyze the formation of M2 with K_m, V_{max}, K_{si}, and CL_{int} at 0.41 ± 0.04 μM, 240.30 ± 7.05 pmol/min/mg, 139.30 ± 29.46 μM, and 586.10 μL/min/mg, respectively, but showed a low activity toward M1 formation. UGT1A9 exhibited a high affinity (K_m, 0.40 ± 0.14 μM) and capacity (V_{max}, 14734.00 ± 1811.00 pmol/min/mg) toward the

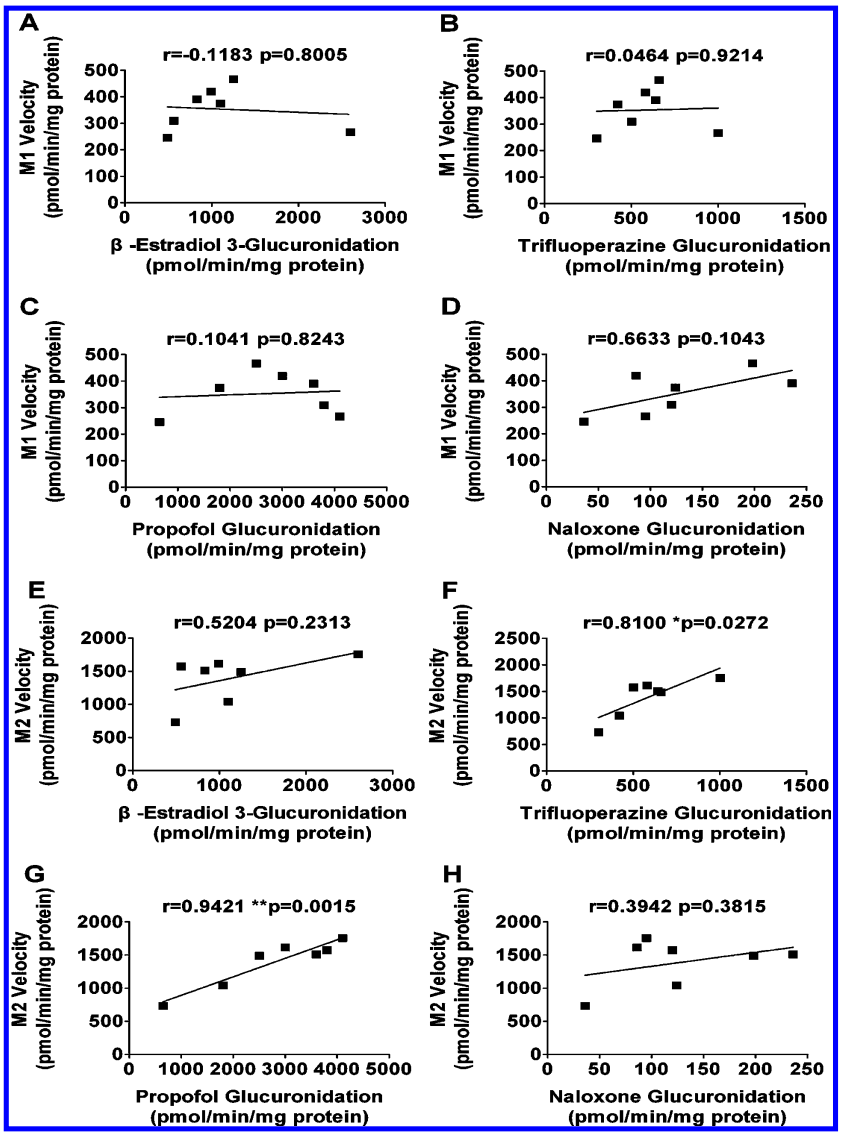

Figure 5. Correlation analysis of β-Lap glucuronidation with the typical UGT1A1 (estradiol, A and E), 1A4 (trifluoperazine, B and F), 1A9 (propofol, C and G), and 2B7 (naloxone, D and H) substrates in 7 individual human liver microsomes in combination with pooled human liver cytosol as an NQO1 donor. A p value less than 0.05 was considered statistically significant.

formation of M2, while UGT1A7 and UGT1A8 exhibited a moderate affinity and capacity. In contrast, UGT2B7 preferred to produce M1 with the apparent kinetic parameter K_m, V_{max}, K_{si}, and CL_{int} at 19.30 ± 6.04 μM, 21125.00 ± 5765.00 pmol/min/mg, 3.04 ± 0.97 μM, and 1094.56 μL/min/mg, respectively.

Enzymatic and Nonenzymatic Reduction of β-Lap. To determine the role of NQO1 on reducing β-Lap, enzymatic and nonenzymatic reduction assays were conducted in recombinant human UGT1A9 and UGT2B7 with or without the addition of recombinant human NQO1 and NADPH generation system (Table 3). It was surprising to find that β-Lap underwent quinone reduction and subsequent glucuronidation metabolism even without the addition of both NQO1 and NADPH albeit to a very weak metabolism, suggesting a nonenzymatic reduction. Furthermore, the addition of NADPH could significantly promote the nonenzymatic reduction, and the enzymatic activity of NQO1 was found largely dependent on the addition of NADPH. As expected, the metabolic velocity was highest when both NQO1 and NADPH were concurrently added. For UGT1A9, the velocities of M1 and M2 formation in the group with the addition of both NADPH and NQO1 were 11.2- and 7.7-fold, respectively, higher than that where only NADPH was added. For UGT2B7, such a difference was 51.0- and 25.7-fold, respectively. These results strongly suggest that NQO1 plays an important role in promoting the reduction and subsequent glucuronidation of β-Lap; however, β-Lap can also be reduced in an NQO1 independent and NADPH facilitated manner.

■ DISCUSSION

High expression levels of NQO1 have been observed in liver, lung, colon, and breast tumors as compared to normal tissues of the same origin.[20,21] In particular, NQO1 activity was increased up to 80-fold in non-small cell lung carcinoma (NSCLC) tumors relative to normal lung and 20−35-fold in NSCLC relative to small cell lung carcinomas (SCLC) cell lines.[22]

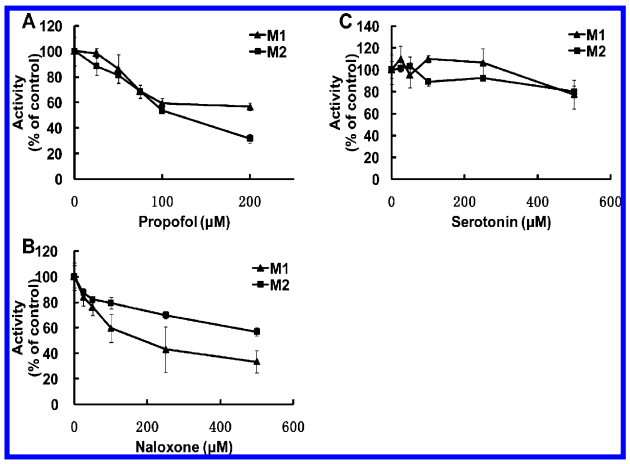

Figure 6. Inhibitory effects of typical substrates on β-Lap glucuronidation in pooled human liver S9. Propofol (0−200 μM), naloxone (0−500 μM), and serotonin (0−500 μM) were used as inhibitors. The protein concentration was 0.025 mg/mL protein, and the incubation time was 10 min. IC50 values were calculated graphically, and each data point represents the mean of triplicate incubations.

The distinctive higher expression levels of NQO1 in various tumor tissues relative to the normal tissues promise NQO1 as a potential therapeutic target.[23] β-Lap is a promising NQO1 target antitumor drug candidate. Its pharmacological activity and involved mechanisms have been extensively studied. In contrast, much less is known about its metabolic properties and mechanisms. A number of previous researches have contributed to the metabolite identification of β-Lap and indicated that β-Lap is predominately metabolized via quinone reduction and subsequent glucuronidation.[12] However, critical questions concerning the metabolism of β-Lap including the enzymes involved in the reduction and glucuronidation and the enzymatic kinetics remain elusive. The present study contributed to a novel and important finding that NQO1 and UGT1A9/UGT2B7 mediated quinone reduction and subsequent glucurondiation are the major determinant of β-Lap metabolism.

On the basis of a LC-IT-TOF/MS analysis and the evidence from the β-glucuronidase enzyme hydrolysis and dicoumarol inhibition experiments, we confirmed that the quinone reduction and subsequent monoglucuronidation to produce a pair of regioisomers (Figure 1, M1 and M2) is the predominant metabolic pathway of β-Lap in human liver and intestinal S9 fractions. This result was consistent with that from previous studies in human hepatocytes and in vivo study. Four other metabolites including three glucuronides (M3, M4, and M5) and one oxidation metabolite (M6) were identified from the human liver S9 incubations. M6, proposed as a dicarboxylic acid metabolite, was previously identified from the whole blood incubations but not human hepatocytes. Our study in human liver S9 fractions suggests that β-Lap can also be oxidized in the liver, albeit to a much lesser extent compared to glucuronidations. M3 and M4 shared the same molecular weight, and both were proposed as the metabolites of hydroxylation in combination with glucuronidation. With the aid of detailed fragment analysis, we were able to propose the different metabolic moiety of M3 and M4; and these two isomers are novel metabolites identified for β-Lap.

To identify the specific UGT isozymes responsible for β-Lap glucuronidation, multiple approaches including reaction phenotyping using recombinant cDNA-expressed UGT enzymes, correlation analysis in human liver microsomes, and chemical inhibition were employed. In vitro incubation with a panel of 12 commercially available human recombinant UGTs supersomes showed that UGT2B7 exhibited the highest activity for the formation of M1, while UGT1A7, UGT1A8, and UGT1A9 were the major isoforms involved in the formation of M2. Results obtained from the present study in combination with previous reports strongly indicates that the ortho-quinone reduction and subsequent glucuronidation is the predominant

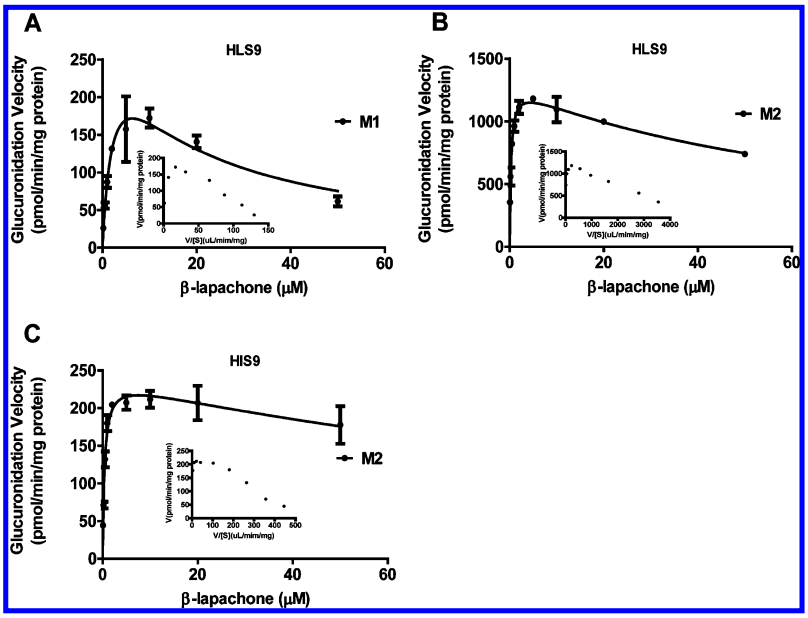

Figure 7. Representative Lineweaver−Burk plots and Eadie−Hofstee plots for the formation of β-Lap glucuronides M1 and M2 by the incubation of β-Lap with HLS9 (A and B) and HIS9 (C). β-Lap (0.1−50 μM) was incubated with HLS9 (0.025 mg/mL) and HIS9 (0.1 mg/mL) for 10 min. Data represent the mean ± SD of triplicate determinations.

dx.doi.org/10.1021/mp300296m | *Mol. Pharmaceutics* 2012, 9, 3476−3485

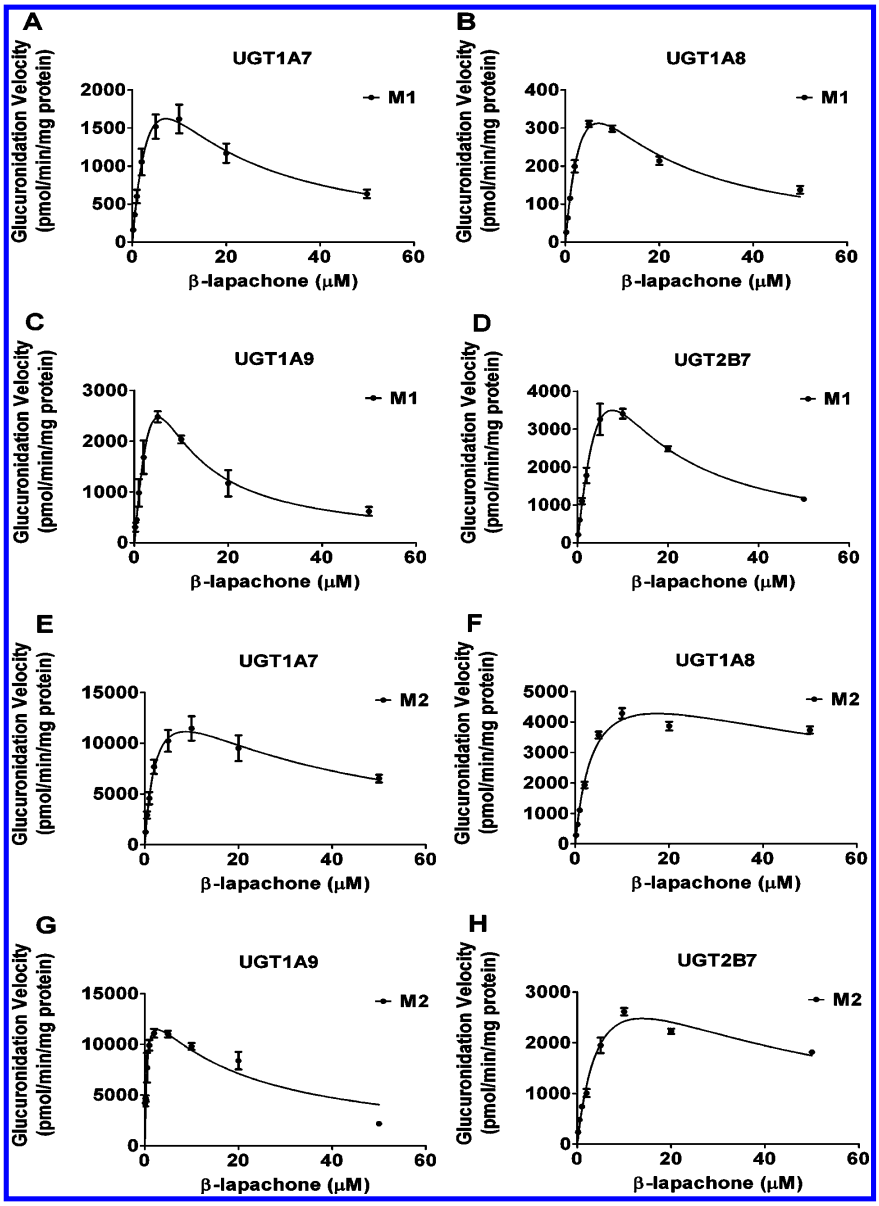

Figure 8. Representative Lineweaver–Burk plots for the formation of *β*-Lap glucuronides (M1 and M2) by incubating *β*-Lap (0.1–50 *μ*M) with the recombinant human UGT1A7 (A and E), UGT1A8 (B and F), UGT1A9 (C and G), and UGT2B7 (D and H) in combination with pooled human liver cytosol as an NQO1 donor.

Table 2. Kinetic Parameters of *β*-Lap Glucuronidations in Pooled Human Liver, Intestinal S9, and Human UGT1A7, UGT1A8, UGT1A9, UGT2B7 Supersomes

	K_m (*μ*mol/L)		V_{max} (pmol/min/mg)		K_{si} (*μ*mol/L)		CL_{int} (*μ*L/min/mg)	
	M1	M2	M1	M2	M1	M2	M1	M2
HLS9	2.37 ± 0.67	0.28 ± 0.02	299.40 ± 46.53	1296.00 ± 23.50	17.07 ± 5.37	68.43 ± 6.31	126.33	4628.57
HIS9	LA	0.41 ± 0.04	LA	240.30 ± 7.05	LA	139.30 ± 29.46	LA	586.10
UGT1A7	5.64 ± 0.91	2.71 ± 0.32	4175.00 ± 468.20	18037.00 ± 1089.00	9.08 ± 1.55	28.32 ± 3.95	740.25	6655.72
UGT1A8	5.78 ± 1.55	4.02 ± 1.10	825.60 ± 156.50	6252.00 ± 840.30	8.58 ± 2.44	75.50 ± 32.46	142.84	1555.22
UGT1A9	37.42 ± 47.13	0.40 ± 0.14	38394.00 ± 46028.00	14734.00 ± 1811.00	0.71 ± 0.89	19.11 ± 6.81	1026.03	36835.00
UGT2B7	19.30 ± 6.04	5.53 ± 1.90	21125.00 ± 5765.00	4458.00 ± 877.70	3.04 ± 0.97	34.60 ± 14.54	1094.56	806.15

metabolic pathway of *β*-Lap, and also other ortho-quinones such as tanshinone IIA.[24] This type of metabolism involves a first step of two-electron reduction to produce a catechol intermediate which is subjected to immediate glucuronidation. Although the two-electron reduction can occur automatically in a nonenzymatic mode for some quinones, this process is greatly promoted by the two-electron quinone reduction enzyme NQO1. Previous studies in assessing the pharmacological mechanisms of

Table 3. Glucuronidation Velocity Followed with Enzymatic and Nonenzymatic Reduction of β-Lap

UGTs	glucuronidation velocity (pmol/min/mg of protein)							
	+NQO1 + NADP		+NQO1 − NADP		−NQO1 + NADP		−NQO1 − NADP	
	M1	M2	M1	M2	M1	M2	M1	M2
UGT1A9	492.06 ± 22.53	7166.74 ± 373.68	0	113.90 ± 0.95	43.90 ± 3.09	934.32 ± 46.30	0	52.61 ± 6.79
UGT2B7	1896.37 ± 45.44	870.56 ± 13.25	2.20 ± 0.07	2.00 ± 0.18	37.22 ± 2.75	33.89 ± 1.39	1.13 ± 0.20	1.00 ± 0.22

β-Lap strongly indicate that NQO1 playes a pivotal role on initiating a redox cycle, hinting to the potential role of NQO1 in β-Lap metabolism.[10,13,25] In the present study, we have confirmed that the addition of recombinant NQO1 can dramatically promote the glucuronidations of β-Lap, although nonenzymatic reduction of β-Lap was found. For this consideration, we employed pooled human liver cytosol as an NQO1 donor to conduct the UGT screening and followed enzyme kinetics assay to mimic in vivo conditions. Results from the reaction phenotyping assay suggest UGT1A7, 1A8, 1A9, and 2B7 are the major isoforms involved in β-Lap glucuronidations. With great benefit from the recent study in the absolute levels of various UGT isoforms in humans,[26] it will be possible to assess the quantitative contributions of these isoforms to the metabolism of β-Lap in vivo. UGT1A7 is expressed in the proximal tissues of the gastrointestinal tract; UGT1A8 is expressed in human jejunum and ileum;[27] both UGT1A7 and 1A8 are nondetectable in the liver. In contrast, the level of UGT1A9 in the liver is much higher than that in the intestine. Thus, it can be proposed that UGT1A7 and 1A8 are the major determinants for β-Lap metabolism in the intestine, while UGT1A9 dominates in the liver. Because UGT1A9 possesses the highest affinity to the metabolism of β-Lap and its absolute level is higher than UGT1A7 and 1A8, liver may possess much stronger activity in metabolizing β-Lap than intestine. Indeed, we found in the enzymatic kinetic analysis that the total CL_{int} (M1 + M2) in HLS9 was 8.1-fold higher than that in HIS9. The formation of M1 was trace and not quantitatively detectable in HIS9, possibly because of the relatively low expression of UGT2B7 in human gastrointestinal tract.[28,29]

To validate the reaction phenotyping results, correlation analysis and chemical inhibition study were further performed. The correlation analysis showed that the formation of M1 and M2 correlated well with naloxone and propofol glucuronidation, respectively, which is consistent with the reaction phenotyping results. The effects of typical substrates including propofol (UGT1A9), naloxone (UGT2B7), and serotonin (UGT1A6) on inhibiting β-Lap glucuronidation were evaluated in HLS9. Naloxone, a specific inhibitor of UGT2B7, exhibited strong inhibition on M1 formation (IC50 = 104.2 ± 1.17 μM). The UGT 1A9 probe propofol decreased both M1 and M2 formation in a concentration-dependent manner with IC50 values of 60.53 ± 1.04 μM and 91.75 ± 1.02 μM, respectively. These results strongly suggest that UGT 2B7 (M1) and UGT1A9 (M2) are the dominant isozymes involved in the metabolism of β-Lap in the liver, while UGT1A7 and 1A8 may be involved in the intestine.

It is very interesting to find that β-Lap can be automatically reduced in a nonenzymatic mode and the autoreduction can be efficiently promoted by NADPH. In contrast, the nonenzymatic autoreduction was not observed in tanshinone IIA, a structural analogue to β-Lap (data not shown). This finding may shed light on understanding the pharmacological properties of β-Lap. It has been well acknowledged that the anticancer effect of β-Lap is largely dependent on the quinone reduction triggered redox cycle. The major limitation of β-Lap as a drug candidate lies in the fact that the specificity and selectivity to NQO1 dependent cytotoxicity can be achieved only within a relatively narrow dose range and short time exposure.[10] Given that NADPH is equally distributed across both tumor cells and normal cells, our finding that NADPH can dramatically trigger the quinone reduction of β-Lap provides a reasonable explanation to the poor NQO1 specificity and the resultant NQO1-irrelevant cytotoxicity of β-Lap at high concentration and prolonged treatment.[10] The future drug design of NQO1 target quinones should be careful to avoid the autoreduction property and thus to increase NQO1 specificity.

In summary, the NQO1-mediated quinone reduction and subsequent glucuronidation represents the major metabolic pathway for β-Lap in human liver and intestine. We demonstrate that UGT1A7, UGT1A8, and UGT1A9 are the predominant isoforms responsible for the formation of M2, while UGT2B7 exhibits the highest activity for the formation of M1. Results obtained from the present study may not only be useful for the understanding of metabolic properties of β-Lap but also shed light on optimizing the strategy to design NQO1 target quinones.

AUTHOR INFORMATION

Corresponding Author

*State Key Laboratory of Natural Medicines, Key Lab of Drug Metabolism and Pharmacokinetics, China Pharmaceutical University, 24 Tong Jia Xiang, Nanjing, China, 210009. H.H.: tel, +86-25-83271179; fax, +86-25-83271060; e-mail, hhp_770505@yahoo.com.cn. G.W.: tel, +86-25-83271128; fax, +86-25-83302827; e-mail, guangjiwang@hotmail.com.

Notes

The authors declare no competing financial interest.

ACKNOWLEDGMENTS

This study was financially supported by a Foundation for the Author of National Excellent Doctoral Dissertation of China (200979), Natural Science Foundation of Jiangsu province (BK2011065), Science Foundation for Youth Scholars of Ministry of Education of China (200803161012), the Program for New Century Excellent Talents in University (NCET-09-0770), and National Natural Science Foundation China (No. 91029746, 30801422).

ABBREVIATIONS USED

β-Lap, β-lapachone; UGT, UDP-glucuronosyltransferase; UDPGA, UDP-glucuronic acid; NQO1, NAD(P)H:quinone oxidoreductase 1; NADP, β-nicotinamide adenine dinucleotide phosphate; LC-IT-TOF/MS, liquid chromatography/hybrid ion trap/time-of-flight mass spectrometry; LC−MS, liquid chromatography−mass spectrometry; HLS9, human liver S9; HIS9, human intestinal S9; HLM, human liver microsome; IC50, inhibitor concentration that causes 50% inhibition; CL_{int}, intrinsic clearance; LA, low activity

REFERENCES

(1) Schaffner-Sabba, K.; Schmidt-Ruppin, K. H.; Wehrli, W.; Schuerch, A. R.; Wasley, J. W. beta-Lapachone: synthesis of derivatives and activities in tumor models. *J. Med. Chem.* **1984**, *27* (8), 990−4.

(2) Cruz, F. S.; Docampo, R.; Boveris, A. Generation of superoxide anions and hydrogen peroxide from beta-lapachone in bacteria. *Antimicrob. Agents Chemother.* **1978**, *14* (4), 630−3.
(3) Medeiros, C. S.; Pontes-Filho, N. T.; Camara, C. A.; Lima-Filho, J. V.; Oliveira, P. C.; Lemos, S. A.; Leal, A. F.; Brandao, J. O.; Neves, R. P. Antifungal activity of the naphthoquinone beta-lapachone against disseminated infection with Cryptococcus neoformans var. neoformans in dexamethasone-immunosuppressed Swiss mice. *Braz. J. Med. Biol. Res.* **2010**, *43* (4), 345−9.
(4) Boveris, A.; Docampo, R.; Turrens, J. F.; Stoppani, A. O. Effect of beta-lapachone on superoxide anion and hydrogen peroxide production in Trypanosoma cruzi. *Biochem. J.* **1978**, *175* (2), 431−9.
(5) Bourguignon, S. C.; Cavalcanti, D. F.; de Souza, A. M.; Castro, H. C.; Rodrigues, C. R.; Albuquerque, M. G.; Santos, D. O.; da Silva, G. G.; da Silva, F. C.; Ferreira, V. F.; de Pinho, R. T.; Alves, C. R. Trypanosoma cruzi: insights into naphthoquinone effects on growth and proteinase activity. *Exp. Parasitol.* **2011**, *127* (1), 160−6.
(6) Pardee, A. B.; Li, Y. Z.; Li, C. J. Cancer therapy with beta-lapachone. *Curr. Cancer Drug Targets* **2002**, *2* (3), 227−42.
(7) Planchon, S. M.; Wuerzberger, S.; Frydman, B.; Witiak, D. T.; Hutson, P.; Church, D. R.; Wilding, G.; Boothman, D. A. Beta-lapachone-mediated apoptosis in human promyelocytic leukemia (HL-60) and human prostate cancer cells: a p53-independent response. *Cancer Res.* **1995**, *55* (17), 3706−11.
(8) Wuerzberger, S. M.; Pink, J. J.; Planchon, S. M.; Byers, K. L.; Bornmann, W. G.; Boothman, D. A. Induction of apoptosis in MCF-7:WS8 breast cancer cells by beta-lapachone. *Cancer Res.* **1998**, *58* (9), 1876−85.
(9) Huang, L.; Pardee, A. B. beta-lapachone induces cell cycle arrest and apoptosis in human colon cancer cells. *Mol. Med.* **1999**, *5* (11), 711−20.
(10) Bey, E. A.; Bentle, M. S.; Reinicke, K. E.; Dong, Y.; Yang, C. R.; Girard, L.; Minna, J. D.; Bornmann, W. G.; Gao, J.; Boothman, D. A. An NQO1- and PARP-1-mediated cell death pathway induced in non-small-cell lung cancer cells by beta-lapachone. *Proc. Natl. Acad. Sci. U.S.A.* **2007**, *104* (28), 11832−7.
(11) Rich, T.; Allen, R. L.; Wyllie, A. H. Defying death after DNA damage. *Nature* **2000**, *407* (6805), 777−83.
(12) Miao, X. S.; Zhong, C.; Wang, Y.; Savage, R. E.; Yang, R. Y.; Kizer, D.; Volckova, E.; Ashwell, M. A.; Chan, T. C. In vitro metabolism of beta-lapachone (ARQ 501) in mammalian hepatocytes and cultured human cells. *Rapid Commun. Mass Spectrom.* **2009**, *23* (1), 12−22.
(13) Pink, J. J.; Planchon, S. M.; Tagliarino, C.; Varnes, M. E.; Siegel, D.; Boothman, D. A. NAD(P)H:Quinone oxidoreductase activity is the principal determinant of beta-lapachone cytotoxicity. *J. Biol. Chem.* **2000**, *275* (8), 5416−24.
(14) Bentle, M. S.; Reinicke, K. E.; Bey, E. A.; Spitz, D. R.; Boothman, D. A. Calcium-dependent modulation of poly(ADP-ribose) polymerase-1 alters cellular metabolism and DNA repair. *J. Biol. Chem.* **2006**, *281* (44), 33684−96.
(15) Miao, X. S.; Song, P.; Savage, R. E.; Zhong, C.; Yang, R. Y.; Kizer, D.; Wu, H.; Volckova, E.; Ashwell, M. A.; Supko, J. G.; He, X.; Chan, T. C. Identification of the in vitro metabolites of 3,4-dihydro-2,2-dimethyl-2H-naphthol[1,2-b]pyran-5,6-dione (ARQ 501; beta-lapachone) in whole blood. *Drug Metab. Dispos.* **2008**, *36* (4), 641−8.
(16) Savage, R. E.; Tyler, A. N.; Miao, X. S.; Chan, T. C. Identification of a novel glucosylsulfate conjugate as a metabolite of 3,4-dihydro-2,2-dimethyl-2H-naphtho[1,2-b]pyran-5,6-dione (ARQ 501, beta-lapachone) in mammals. *Drug Metab. Dispos.* **2008**, *36* (4), 753−8.
(17) Wang, Q.; Hao, H.; Zhu, X.; Yu, G.; Lai, L.; Liu, Y.; Wang, Y.; Jiang, S.; Wang, G. Regioselective glucuronidation of tanshinone iia after quinone reduction: identification of human UDP-glucuronosyltransferases, species differences, and interaction potential. *Drug Metab. Dispos.* **2010**, *38* (7), 1132−40.
(18) Talcott, R. E.; Rosenblum, M.; Levin, V. A. Possible role of DT-diaphorase in the bioactivation of antitumor quinones. *Biochem. Biophys. Res. Commun.* **1983**, *111* (1), 346−51.
(19) Reber, P.; Brenneisen, R.; Flogerzi, B.; Batista, C.; Netzer, P.; Scheurer, U. Effect of naloxone-3-glucuronide and N-methylnaloxone on the motility of the isolated rat colon after morphine. *Dig. Dis. Sci.* **2007**, *52* (2), 502−7.
(20) Belinsky, M.; Jaiswal, A. K. NAD(P)H:quinone oxidoreductase1 (DT-diaphorase) expression in normal and tumor tissues. *Cancer Metastasis Rev.* **1993**, *12* (2), 103−17.
(21) Smitskamp-Wilms, E.; Giaccone, G.; Pinedo, H. M.; van der Laan, B. F.; Peters, G. J. DT-diaphorase activity in normal and neoplastic human tissues; an indicator for sensitivity to bioreductive agents? *Br. J. Cancer* **1995**, *72* (4), 917−21.
(22) Malkinson, A. M.; Siegel, D.; Forrest, G. L.; Gazdar, A. F.; Oie, H. K.; Chan, D. C.; Bunn, P. A.; Mabry, M.; Dykes, D. J.; Harrison, S. D.; et al. Elevated DT-diaphorase activity and messenger RNA content in human non-small cell lung carcinoma: relationship to the response of lung tumor xenografts to mitomycin Cl. *Cancer Res.* **1992**, *52* (17), 4752−7.
(23) Liu, F.; Yu, G.; Wang, G.; Liu, H.; Wu, X.; Wang, Q.; Liu, M.; Liao, K.; Wu, M.; Cheng, X.; Hao, H. An NQO1-initiated and p53-independent apoptotic pathway determines the anti-tumor effect of tanshinone IIA against non-small cell lung cancer. *PLoS One* **2012**, *7* (7), e42138.
(24) Hao, H.; Wang, G.; Cui, N.; Li, J.; Xie, L.; Ding, Z. Identification of a novel intestinal first pass metabolic pathway: NQO1 mediated quinone reduction and subsequent glucuronidation. *Curr. Drug Metab.* **2007**, *8* (2), 137−49.
(25) Choi, E. K.; Terai, K.; Ji, I. M.; Kook, Y. H.; Park, K. H.; Oh, E. T.; Griffin, R. J.; Lim, B. U.; Kim, J. S.; Lee, D. S.; Boothman, D. A.; Loren, M.; Song, C. W.; Park, H. J. Upregulation of NAD(P)H:quinone oxidoreductase by radiation potentiates the effect of bioreductive beta-lapachone on cancer cells. *Neoplasia* **2007**, *9* (8), 634−42.
(26) Harbourt, D. E.; Fallon, J. K.; Ito, S.; Baba, T.; Ritter, J. K.; Glish, G. L.; Smith, P. C. Quantification of human uridine-diphosphate glucuronosyl transferase 1A isoforms in liver, intestine, and kidney using nanobore liquid chromatography-tandem mass spectrometry. *Anal. Chem.* **2012**, *84* (1), 98−105.
(27) Tukey, R. H.; Strassburg, C. P. Human UDP-glucuronosyltransferases: metabolism, expression, and disease. *Annu. Rev. Pharmacol. Toxicol.* **2000**, *40*, 581−616.
(28) Nakamura, A.; Nakajima, M.; Yamanaka, H.; Fujiwara, R.; Yokoi, T. Expression of UGT1A and UGT2B mRNA in human normal tissues and various cell lines. *Drug Metab. Dispos.* **2008**, *36* (8), 1461−4.
(29) Ohno, S.; Nakajin, S. Determination of mRNA expression of human UDP-glucuronosyltransferases and application for localization in various human tissues by real-time reverse transcriptase-polymerase chain reaction. *Drug Metab. Dispos.* **2009**, *37* (1), 32−40.